SPACIAL ENERGY FLOW DISTRIBUTION ON THREE–PHASE HIGH–VOLTAGE LINES

H. Grabinski[1]* and F. Wiznerowicz[2]
[1]Leibniz Universität Hannover, LFI, Schneiderberg 32, 30167 Hannover, Germany
[2]Fachhochschule Hannover, Ricklinger Stadtweg 120, 30459 Hannover, Germany
*Email: <grabinski@lfi.uni-hannover.de>

Abstract: The spacial energy flow distribution on three–phase high–voltage lines was analyzed using the Poynting vector. Thereby it appeared that in spite of reactive loads there are regions in space — dependent on whether the loads are balanced or not — where the time averaged Poynting vector does *not* vanish. That means that in these regions in case of pure reactive loads active power is transmitted.

1 INTRODUCTION

It is the intention of this paper to answer the question how in detail energy transfer takes place along a three–phase high-voltage power line. The general way to calculate the active power transportation along a power line with lines numbered by L1, L2 and L3 is quite simple and well known already for undergraduate students: Using the delta voltages U_{12}, U_{23} and U_{31} (root-mean-square values) as well as the (in general: complex) delta-loads $\underline{Y}_{12}$, $\underline{Y}_{23}$ and $\underline{Y}_{31}$, the active power can be calculated by

$$P = U_{12}^2 \mathfrak{Re}\{\underline{Y}_{12}\} + U_{23}^2 \mathfrak{Re}\{\underline{Y}_{23}\} + U_{31}^2 \mathfrak{Re}\{\underline{Y}_{31}\} \quad (1)$$

neglecting all line losses. In addition one can see, if all loads are pure reactive, no active power is transmitted. But using (1) one cannot see at all *how* the active power transportation will take place in detail.

To investigate the latter, the most suitable and powerful quantity is the Poynting vector $\boldsymbol{S}(\boldsymbol{r}, t)$ which was introduced in 1884 by John Henry Poynting. It describes the energy flow with respect of magnitude and direction of an electromagnetic field in terms of a power density and is defined to be (cf. e.g. [1])

$$\boldsymbol{S}(\boldsymbol{r}, t) = \boldsymbol{E}(\boldsymbol{r}, t) \times \boldsymbol{H}(\boldsymbol{r}, t) . \quad (2)$$

Herein the vectors $\boldsymbol{E}$ and $\boldsymbol{H}$ represent the electric as well as the magnetic field strength, the vector $\boldsymbol{r}$ is the position in space and t is the time.

For the calculation of the power transmitted through an arbitrary surface A_S, we have to integrate $\boldsymbol{S}(\boldsymbol{r}, t)$ over this surface, i.e. $\int_{A_S} \boldsymbol{S}(\boldsymbol{r}, t)\, \mathrm{d}\boldsymbol{A}$. Applied to straight power lines, we obtain the (instantaneous) value of the overall transmitted power $p(t)$ by integration of $\boldsymbol{S}(\boldsymbol{r}, t)$ over an infinite cross–sectional area *perpendicular* to the power lines,

$$p(t) = \int_{-\infty}^{+\infty} \int_{-\infty}^{+\infty} \boldsymbol{S}(x, y, t)(\boldsymbol{e}_x \times \boldsymbol{e}_y)\, \mathrm{d}x\, \mathrm{d}y . \quad (3)$$

Herein $\boldsymbol{e}_x$ and $\boldsymbol{e}_y$ are the unit vectors in x– and y–direction as well. What we finally need is the transmitted *active* power P which is the time averaged value of $p(t)$, indicated by an overline, i.e.

$$\begin{aligned} P = \overline{p(t)} &= \frac{1}{T} \int_0^T p(t)\, \mathrm{d}t \\ &= \int_{-\infty}^{+\infty} \int_{-\infty}^{+\infty} \overline{\boldsymbol{S}(x, y, t)}(\boldsymbol{e}_x \times \boldsymbol{e}_y)\, \mathrm{d}x\, \mathrm{d}y . \end{aligned} \quad (4)$$

The description of energy transmission using $\boldsymbol{S}$ sometimes results in seemingly paradoxical results. For example, since the magnitudes of $\boldsymbol{E}$ and $\boldsymbol{H}$ outside the conductors of a power line are in general much larger than inside the conductors (e.g. there is absolutely no electric field inside *perfect* conducting material) we have to conclude that energy transport takes place nearly *completely* outside (!) the conductors.

In chapter 2 we will derive formulae for calculating the Poynting vector in case of a three–phase line and we will discuss the result. In the scope of this discussion we will come to the conclusion, that in spite of pure reactive loads nevertheless the transmission of active power is possible.

To illustrate this surprising result, in chapter 3 this effect will be demonstrated for a real three phase line system and discussed in more detail in chapter 4. The last chapter is a conclusion.

2 ENERGY TRANSFER ON THREE–PHASE LINES

We consider a three–phase system consisting of three conductors of an overhead line. The three conductors are arranged in form of an equilateral triangle as depicted in fig. 1. The distances l between the conductors are 3,6 m, the line diameters d are 21,8 mm, and the distance h of the center of the triangle to ground is 18,5 m. The maximum rms–value of the steady current for

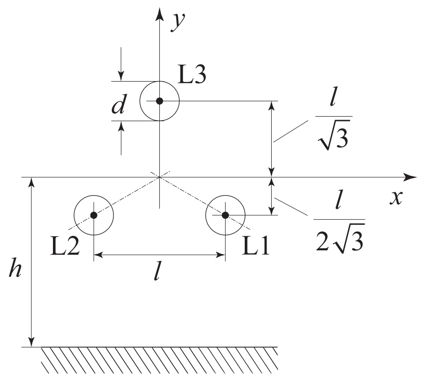

Fig. 1 Three–phase system of an overhead line [2]

each conductor is 645 A, and we assume a delta rms–voltage of $U = 110$ kV i.e. a rms–voltage to neutral of $U_0 = 64$ kV.

To calculate the Poynting vector, we have to calculate the electric and magnetic fields. The general procedure is depicted in fig. 2: Starting with the given geometrical data (cf. fig. 1), the material data ($\epsilon = \epsilon_0$, $\mu = \mu_0$ in the whole space), the voltages (e.g. voltages to neutral $\underline{U}_1 = U_0\,\mathrm{e}^{-\mathrm{j}30^\circ}$, $\underline{U}_2 = U_0\,\mathrm{e}^{-\mathrm{j}150^\circ}$ and $\underline{U}_3 = U_0\,\mathrm{e}^{\mathrm{j}90^\circ}$)

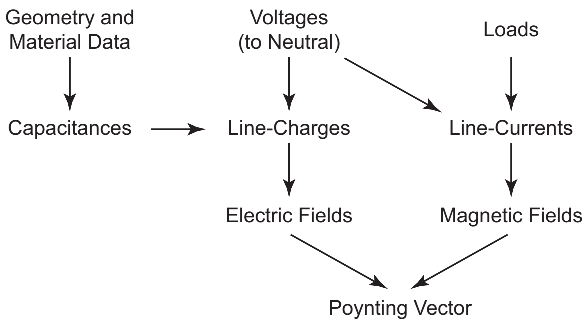

Fig. 2 General calculation procedure

and the loads (e.g. $\underline{Y}_{12}$, $\underline{Y}_{23}$, $\underline{Y}_{31}$), one can calculate capacitances, line–charges $q_i'(t)$ per unit length (p.u.l.) and line–currents $i_k(t)$, the electric and magnetic fields and finally the Poynting vector.

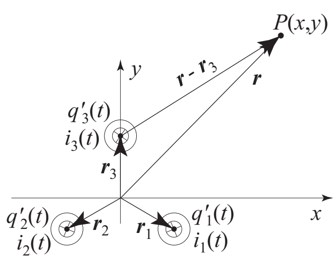

Fig. 3 System of three lines represented by charges and currents (image charges are not depicted)

The resulting electric as well as magnetic field at an arbitrary point $P(x,y)$, described by the vectors $\boldsymbol{r}$ and $\boldsymbol{r}_1$ to $\boldsymbol{r}_3$ (fig. 3), is then a linear superposition of the individual fields of each conductor (plus the electric fields of image charges), i.e.

$$\boldsymbol{E}(P,t) = \sum_{i=1}^{3} \boldsymbol{E}_i(P,t) + \boldsymbol{E}_{i\,img}(P,t) \qquad (5)$$

and

$$\boldsymbol{H}(P,t) = \sum_{k=1}^{3} \boldsymbol{H}_k(P,t)\,, \qquad (6)$$

where the mentioned individual fields are simply the electric fields of the straight line charges $q_i'(t)$ p.u.l. as well as the magnetic fields of the line currents $i_k(t)$ with e.g. $i,k = 1,2,3$ for the depicted three–phase system (c.f. fig. 3).

Assuming that $q_i'(t)$ and $i_k(t)$ are sinusoidal functions with respect to time, i.e.

$$q_i'(t) = \hat{q}_i'\,\cos(\omega t + \varphi_i) \qquad (7)$$

$$i_k(t) = \hat{i}_k\,\cos(\omega t + \psi_k), \quad i,k = 1\ldots 3\,, \qquad (8)$$

with ω = angular frequency of charges and currents, then for the three–phase system of fig. 3 we obtain for every single point P in space rotating electric and magnetic field vectors, describing elliptic curves as depicted in fig. 4. Herein the angular velocities $\omega_E(P,t)$ and $\omega_H(P,t)$ of the field vectors $\boldsymbol{E}(P,t)$ and $\boldsymbol{H}(P,t)$ are in general not only different from each other (and sometimes contra-rotating), but also functions of time, depending on the position P in space and on the values of the loads $\underline{Y}_{12}$, $\underline{Y}_{23}$ and $\underline{Y}_{31}$, respectively. As

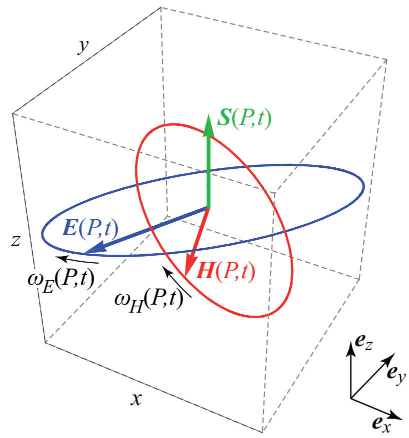

Fig. 4 Field vectors $\boldsymbol{E}(P,t)$ and $\boldsymbol{H}(P,t)$, rotating in the x–y–plane, and Poynting vector $\boldsymbol{S}(P,t) = S_z(P,t)\boldsymbol{e}_z$. $\omega_E(P,t)$ and $\omega_H(P,t)$ are the angular velocities of the field vectors with in general $\omega_E(P,t) \neq \omega_H(P,t)$.

an example: If $\hat{E}_x(P)$ and $\hat{E}_y(P)$ are the respective peak-values of the x– and y–components of $\boldsymbol{E}(P,t)$, and $\varphi_{E\,x}(P)$ and $\varphi_{E\,y}(P)$ are the corresponding phase angles, then the angular velocity $\omega_E(P,t)$ equals

$$\omega_E(P,t) = \omega\,\frac{\hat{E}_x(P)\hat{E}_y(P)\,\frac{\sin\left(\varphi_{E\,y}(P)-\varphi_{E\,x}(P)\right)}{\cos^2\left(\omega t+\varphi_{E\,y}(P)\right)}}{\hat{E}_y(P)^2 + \hat{E}_x(P)^2\,\frac{\cos^2\left(\omega t+\varphi_{E\,x}(P)\right)}{\cos\left(\omega t+\varphi_{E\,y}(P)\right)}}\,, \qquad (9)$$

similarly for $\omega_H(P,t)$. Figure 5 shows a typical curve shape of $\omega_E(P,t)$. The angular frequency ω is the

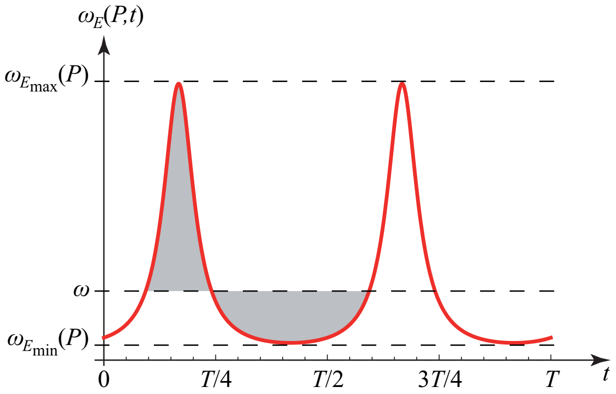

Fig. 5 Typical curve shape of $\omega_E(P,t)$. The arithmetic average of the angular velocity $\omega_E(P,t)$ (as well as of $\omega_H(P,t)$) is equal to the angular frequency ω.

arithmetic average of the angular velocity $\omega_E(P,t)$ with respect to time: The two shaded regions in fig. 5 have the same size.

From (2) together with (5) and (6), for the Poynting vector we obtain

$$\boldsymbol{S}(P,t) = \sum_{i=1}^{3}\sum_{k=1}^{3} \underbrace{\left[\boldsymbol{E}_i(P,t) + \boldsymbol{E}_{i\,img}(P,t)\right] \times \boldsymbol{H}_k(P,t)}_{=:\boldsymbol{S}_{ik}(P,t)}, \tag{10}$$

and since all field–components $\boldsymbol{E}_i(P,t)$, $\boldsymbol{E}_{i\,img}(P,t)$ and $\boldsymbol{H}_k(P,t)$ of $\boldsymbol{E}(P,t)$ and $\boldsymbol{H}(P,t)$ are located exclusively in the x–y–plane, all parts $\boldsymbol{S}_{ik}(P,t) = \left[\boldsymbol{E}_i(P,t) + \boldsymbol{E}_{i\,img}(P,t)\right] \times \boldsymbol{H}_k(P,t)$ of $\boldsymbol{S}(P,t)$ must be vectors in the z–direction, i.e. $\boldsymbol{S}_{ik}(P,t) = S_{ik}(P,t)\,\boldsymbol{e}_z$, where $\boldsymbol{e}_z$ is a unit–vector in z–direction (cf. fig. 4).

Taking into consideration (7) and (8) for the calculation of the electric and magnetic fields and after some »smart« manipulations of (10), one gets [3]

$$\boldsymbol{S}(P,t) = -\sum_{i,k=1}^{3} \frac{q_i'(t) i_k(t)}{4\pi^2\epsilon_0} \, \frac{(\boldsymbol{r}-\boldsymbol{r}_i)(\boldsymbol{r}-\boldsymbol{r}_k)}{(\boldsymbol{r}-\boldsymbol{r}_i)^2(\boldsymbol{r}-\boldsymbol{r}_k)^2}\, \boldsymbol{e}_z \,. \tag{11}$$

For calculation of the energy flow distribution and in accordance with (4), finally we need the time average value of $\boldsymbol{S}(P,t)$, i.e.

$$\overline{\boldsymbol{S}(P,t)} = \frac{1}{T}\int_0^T \sum_{i,k=1}^{3} \boldsymbol{S}_{ik}(P,t)\,\mathrm{d}t \,,$$

in which T is the periodic time with $T = \frac{2\pi}{\omega}$. Due to the linearity of integration the averaging process can be reduced to the product terms $q_i'(t) i_k(t)$ in (11), i.e.

$$\begin{aligned} \overline{\boldsymbol{S}(P,t)} &= \sum_{i,k=1}^{3} \overline{S_{ik}(P,t)}\,\boldsymbol{e}_z \\ &= -\sum_{i,k=1}^{3} \frac{\overline{q_i'(t) i_k(t)}}{\dots} \dots \boldsymbol{e}_z \,. \end{aligned} \tag{12}$$

Inserting the right hand terms of (7) and (8) one gets

$$\begin{aligned} \overline{q_i'(t) i_k(t)} &= \hat{q}_i'\,\hat{i}_k\,\overline{\cos(\omega t+\varphi_i)\,\cos(\omega t+\psi_k)} \\ &= \frac{1}{2}\hat{q}_i'\,\hat{i}_k\,\cos(\varphi_i - \psi_k) \end{aligned}$$

and finally for $\overline{S_{ik}(P,t)}$ in (12):

$$\overline{S_{ik}(P,t)} = -\frac{\hat{q}_i'\,\hat{i}_k}{8\pi^2\epsilon_0}\cos(\varphi_i-\psi_k)\,\frac{(\boldsymbol{r}-\boldsymbol{r}_i)(\boldsymbol{r}-\boldsymbol{r}_k)}{(\boldsymbol{r}-\boldsymbol{r}_i)^2(\boldsymbol{r}-\boldsymbol{r}_k)^2} \tag{13}$$

Taking into consideration all combinations of indexes ik, (13) represents 3^2 single equations. But due to the symmetry of the right–most term in (13) with respect to the indexes i and k it makes sense to split (13) into two parts, namely for $i = k$ and $i \neq k$, and then to combine the expressions for $\overline{S_{ik}(P,t)}$ and $\overline{S_{ki}(P,t)}$,

$$\begin{aligned} \overline{S_{ii}(P,t)} &= -\frac{\hat{q}_i'\,\hat{i}_i}{8\pi^2\epsilon_0}\,\frac{\cos(\varphi_i-\psi_i)}{(\boldsymbol{r}-\boldsymbol{r}_i)^2} \\ \overline{S_{ik}(P,t)} &+ \overline{S_{ki}(P,t)} \\ &= -\frac{1}{8\pi^2\epsilon_0}\Big[\hat{q}_i'\,\hat{i}_k\,\cos(\varphi_i-\psi_k) \\ &\quad +\hat{q}_k'\,\hat{i}_i\,\cos(\varphi_k-\psi_i)\Big]\,\frac{(\boldsymbol{r}-\boldsymbol{r}_i)(\boldsymbol{r}-\boldsymbol{r}_k)}{(\boldsymbol{r}-\boldsymbol{r}_i)^2(\boldsymbol{r}-\boldsymbol{r}_k)^2}\,. \end{aligned} \tag{14}$$

For the general case of n lines, (14) represents a maximum of only $n + \frac{n^2-n}{2} = \frac{n(n+1)}{2}$ equations (If in the case of n conductors only $m < n$ conductors are current–carrying, (14) reduces to only $m + \left[\frac{m^2-m}{2} + (n-m)m\right] = \frac{m(2n+1-m)}{2}$ equations.).

Together with the first part of (12), equations (14) represent the general solution for the calculation of the Poynting vector.

Assuming now again a three–phase system, we discuss (14) for

a) a *complete symmetrical geometry* ($\Rightarrow$ all line-charge magnitudes p.u.l. $\hat{q}_i'$ show the identical value $\hat{q}'$) and

b) a *balanced load* ($\Rightarrow$ all current magnitudes $\hat{i}_k$ show the identical value $\hat{i}$ and the phase-differences $\varphi_k - \psi_k$ show a constant value φ)

leads finally to the results [3]

$$\begin{aligned}\overline{S_{ii}(P,t)} &= -\frac{\hat{q}'\,\hat{i}}{8\pi^2\epsilon_0}\frac{\cos\varphi}{(\boldsymbol{r}-\boldsymbol{r}_i)^2}\\ \overline{S_{ik}(P,t)} + \overline{S_{ki}(P,t)} & \qquad\qquad (15)\\ &= \frac{\hat{q}'\,\hat{i}}{8\pi^2\epsilon_0}\cos\varphi\frac{(\boldsymbol{r}-\boldsymbol{r}_i)(\boldsymbol{r}-\boldsymbol{r}_k)}{(\boldsymbol{r}-\boldsymbol{r}_i)^2(\boldsymbol{r}-\boldsymbol{r}_k)^2}\,.\end{aligned}$$

From (15) we see that for a complex load (i.e. $\cos\varphi \neq 0$) $\overline{\boldsymbol{S}(P,t)} \neq 0$, i.e. active power is transmitted as it must be. A comparison between calculations using (4) (together with (15)) and calculations using (1) shows identical results, as expected. Especially for a pure reactive load (i.e. $\varphi = 90°$) $\overline{\boldsymbol{S}(P,t)}$ disappears for all points P of space, i.e. no active power is transmitted as it is well known for reactive loads.

But a *very strange* result we obtain by examination of the general case described by (14): If we discuss (14) in case of a non–symmetrical geometry (i.e. the $\hat{q}_i'$ are different from each other) and/or a non–balanced load (i.e. the currents are different from each other with respect to magnitude and/or phase behavior), we find out that *even in case of pure reactive loads* (!) there are areas in space where $\overline{\boldsymbol{S}(P,t)}$ is *different from zero*! In terms of physics: There are areas where *active power* is transmitted even though the loads are pure reactive! All this is very general, i.e. it is not restricted to three conductors only.

We will illustrate and discuss this surprising result in the next two chapters.

3 ENERGY TRANSFER FOR *BALANCED* AND *UNBALANCED* LOADS

Using the three–phase system given in fig. 1 on page 2, we will evaluate (14) for different loads. In detail and as an illustration we consider two cases of *balanced* delta loads and one case of *unbalanced* loads of an overhead line according fig. 1:

a) $\underline{Y}_{ik} = \frac{10^{-2}}{3}\Omega^{-1}$ (resistors) $\forall\, i,k$,

b) $\underline{Y}_{ik} = \frac{10^{-2}}{3}\,\mathrm{e}^{-\mathrm{j}90°}\,\Omega^{-1}$ (inductances) $\forall\, i,k$ and

c) $\underline{Y}_{12} = \underline{Y}_{23} = \frac{10^{-2}}{3}\,\mathrm{e}^{\mathrm{j}90°}\,\Omega^{-1}$ (capacitances) and $\underline{Y}_{31} = \frac{10^{-2}}{3}\,\mathrm{e}^{-\mathrm{j}90°}\,\Omega^{-1}$ (inductance)

Figures 6 and 7 show the results for the **balanced** loads: Shown is in each case the x–y–plane together with the positions of the lines (black drawn circles) and at different points P around the lines the appropriate plots of the (normalized) Poynting vectors $\boldsymbol{S}(P,t)\boldsymbol{e}_z$ vs. time in figs. 6(a) and 7(a). In addition, the associated time–averaged Poynting vectors $S = \overline{S_z(P,t)}$ are depicted in figs. 6(b) and 7(b).

In fig. 6(a), at each point in time and space the Pointing vectors are greater than or equal zero. That means that in the whole space around the lines active power is transmitted to the loads since the time–averaged Poynting vectors $S = \overline{S_z(P,t)}$ are larger than zero (fig. 6(b)). This is the result we expect for pure active loads.

In fig. 7(a), at each point in time and space the Pointing vectors oscillate around the t–axis. That means that in the whole space around the lines no active power is transmitted to the loads since the time–averaged Poynting vectors $S = \overline{S_z(P,t)}$ equals zero (fig. 7(b)). This is the result we expect for pure reactive loads.

But in a complete contrast to the previous results is the outcome in case of pure reactive but now **unbalanced** loads. Figure 8 shows the calculated results for that case: At different points in space the Pointing vectors partially oscillate around the t–axis, partially are shifted towards positive values, partially towards negative values (fig. 8(a)). That means that in the space around the lines partially active power is transmitted **to** the loads and partially **active** power is transmitted **from** the loads to the generator–side (fig. 8(b)).

4 DISCUSSION OF UNBALANCED, PURE REACTIVE LOADS

From (1) it is clear that in the case of pure reactive (balanced or unbalanced) loads no active power is transmitted. But in spite of this, from (14) and from the results of the previous chapter follows that there are some

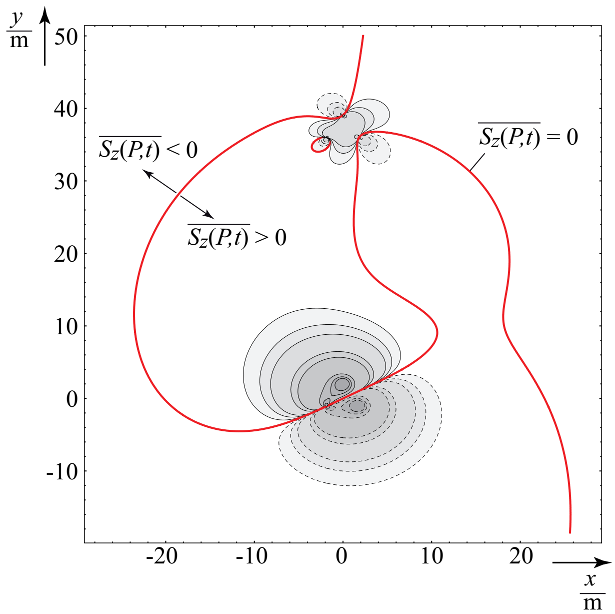

Fig. 9 Lines of constant time-averaged Poynting vectors $\overline{S_z(P,t)}$ in the x-y-plane, corresponding to fig. 8(b) (in the lower part of the plot at about $x = y = 0$ the positions of the three lines are clearly identifiable). The thick red line represents $\overline{S_z(P,t)} = 0$.

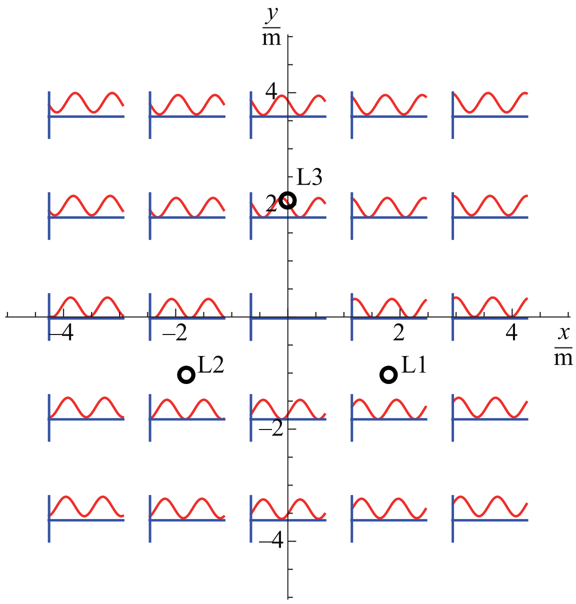

(a) Poynting vectors $\boldsymbol{S}(P,t)\boldsymbol{e}_z$ vs. time at different points P around the lines (black drawn circles)

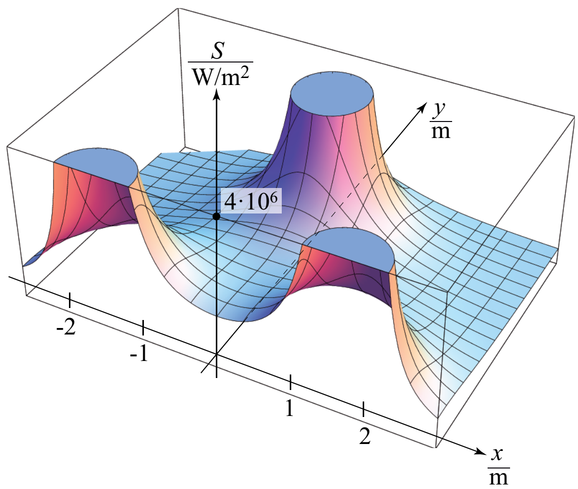

(b) Time–averaged Poynting vector $S = \overline{S_z(P,t)} \geq 0$ in the whole space around the lines

Fig. 6 Poynting vectors for pure **active**, **balanced** loads

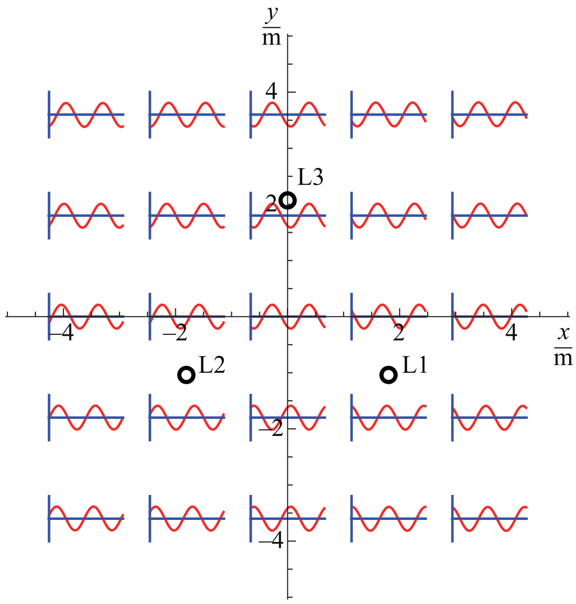

(a) Poynting vectors $\boldsymbol{S}(P,t)\boldsymbol{e}_z$ vs. time at different points P around the lines (black drawn circles)

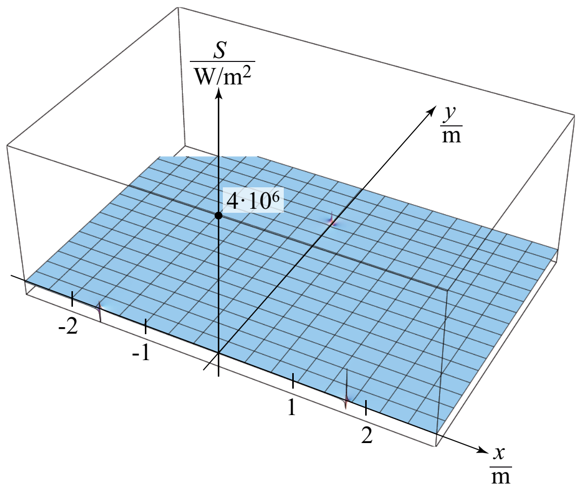

(b) Time–averaged Poynting vector $S = \overline{S_z(P,t)} \equiv 0$ in the whole space around the lines

Fig. 7 Poynting vectors for pure **reactive**, **balanced** loads

few areas of space where $\overline{S_z(P,t)}$ is different from zero and the calculated values are in the same order as in the case of active loads in fig. 6(b).

The difference to fig. 6(b) is, that now there are subareas in fig. 8(b) where $\overline{S_z(P,t)}$ has different directions: partly in the positive z–direction, partly in the negative one. With other words: There are areas where active power is permanently transmitted *to* the reactive loads whereas in other areas the same active power flows permanently *from* the loads *back* to the generator. The latter becomes more clear using a contour plot (fig. 9 on the preceding page): Each curve in the x-y-plane represents the geometric loci of constant values of $\overline{S_z(P,t)}$. At this, the (black) continuous lines represent *positive* values of $\overline{S_z(P,t)}$, the dashed lines *negative* values. The thick red line represents $\overline{S_z(P,t)} = 0$. All this happens — as a matter of course — such way that the overall transmitted active power becomes zero, i.e. $\int_{-\infty}^{\infty}\int_{-\infty}^{\infty} \overline{S_z(P,t)}\,\mathrm{d}x\,\mathrm{d}y = 0$, as it must be.

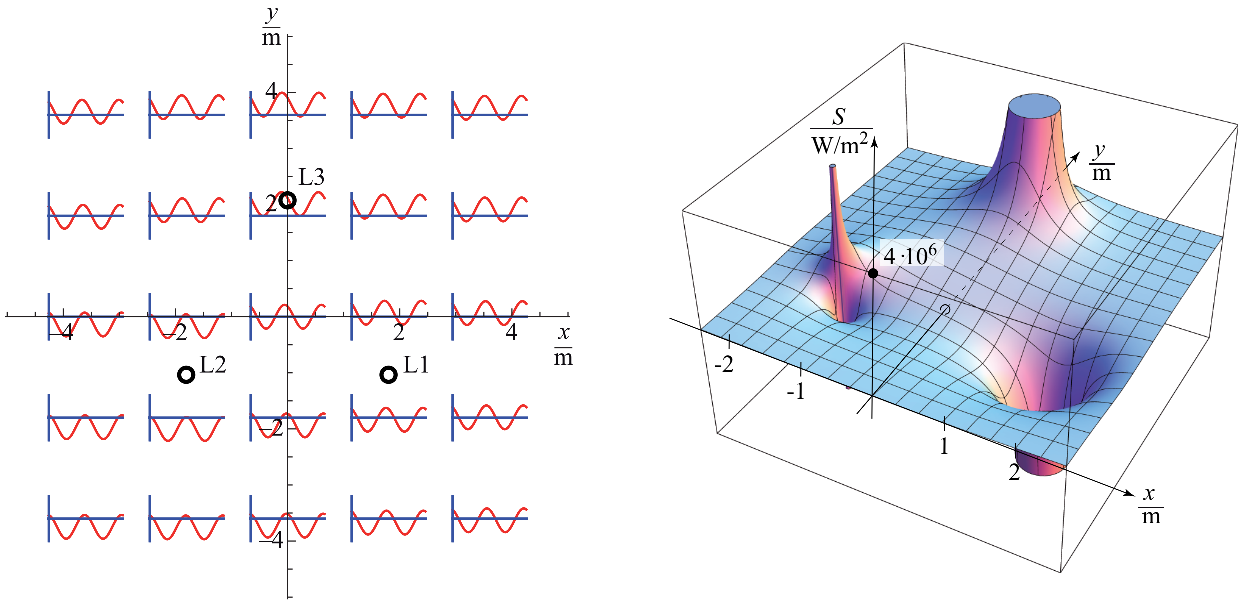

(a) Poynting vectors $\boldsymbol{S}(P,t)\boldsymbol{e}_z$ vs. time at different points P around the lines (black drawn circles)

(b) Time–averaged Poynting vector $S = \overline{S_z(P,t)} > 0$ or < 0 in the space around the lines

Fig. 8 Poynting vectors for pure **reactive**, **un**balanced loads

How do we have to interpret the results above? Why exist areas in space where *permanently* active power is transported *to* or *from* the reactive loads? As a lot of calculations have shown (and as one can be also deduce from (14)), the described behavior is not restricted to our special example: Similar results arise in *all* cases of unbalanced reactive loads, *independent* of the presence of a ground plane or of special geometrical data. It can also be shown that the observed effect arises also for balanced loads but an unsymmetrical geometry what can be deduced from (14), too. A detailed answer to the questions above is given in [3]. Here it should be pointed out only that in case of unbalanced loads or in the case of asymmetric geometries the power will be redirected inside the loads.

5 CONCLUSION

From transmission lines we know that energy transport does not take place *inside* the lines (were especially the electric field is small) but mainly *outside* the lines in the surrounding area. Mathematically (and physically) this is described by the Poynting vector. But the study of energy transfer on three–pase high–voltage lines using the Poynting vector led to a curious result: Even though the load of a three–phase system is *completely reactive*, there can be areas in space where *active power* is transmitted (i.e. the time–averaged Poynting vector is different from zero). Whether or not active power is transmitted depends on whether or not the load is balanced. In case of a *balanced* reactive load *no* active power is transmitted.

In accordance with the fact that neither a balanced nor an unbalanced reactive load can absorb active power, it is arisen from our calculations (in case of unbalanced loads) that in those areas where active power is transmitted *to* the loads the overall power is as much as large as in those areas where active power is transmitted *from* the loads. With other words: In spite of pure reactive loads the generator transmits and receives at the same time but at different spacial positions active power. And that leads to a second curiosity: Only an unbalanced reactive load lets flow back the incoming active power back to the source.

In summary: Since in case of lossless power lines as well as lossless loads no power can be dissipated, for the time–averaged Poynting vector $\overline{\boldsymbol{S}(P,t)}$ holds: $\operatorname{div}\overline{\boldsymbol{S}(P,t)} = 0$.

REFERENCES

[1] J. D. Jackson: "Klassische Elektrodynamik" (de Gruyter, 2002), pp. 300 ff

[2] R. Flosdorff, G. Hilgarth: "Elektrische Energieverteilung" (Vieweg + Teubner, 2005)

[3] H. Grabinski, F. Wiznerowicz: "Energy transfer on three-phase high-voltage lines: the strange behavior of the Poynting vector", Springer, Electrical Engineering Vol. 92, Number 6, pp. 203 – 214, 2010